J. Synchrotron Rad. (1998). **5**, 627–629

Beam-position monitors in the X-ray undulator beamline at PETRA

U. Hahn,* W. Brefeld, M. Hesse, J. R. Schneider, H. Schulte-Schrepping, M. Seebach and M. Werner

Hamburger Synchrotronstrahlungslabor HASYLAB at Deutsches Elektronen Synchrotron DESY, Notkestrasse 85, D-22607 Hamburg, Germany. E-mail: hahn@desy.de

(*Received 4 August 1997; accepted 17 October 1997*)

At the 12 GeV storage ring PETRA, the first synchrotron radiation beamline uses a 4 m-long undulator. The beamline, with a length of 130 m between source and sample, delivers hard X-ray photons usable up to 300 keV. The photon beam has a total power of 7 kW. Combined with the high brilliance, the powerful beam is very critical for all beamline components. Copper, located at a distance of 26 m, hit by the full undulator beam, melts within 20 ms. Different monitors are described for stable, safe and reliable operation of beam and experiments.

Keywords: beam-position monitors; undulators; hard X-rays.

1. Introduction

The 4 m-long X-ray undulator at the 12 GeV storage ring PETRA (Balewski *et al.*, 1995) is a high-brightness synchrotron radiation source (Hahn *et al.*, 1997). The beam is used in the spectral range 16–300 keV with a total power of up to 7 kW. This very powerful undulator beam passes a beamline front end with a total length of 105 m before the beam is simultaneously used at two experimental stations. The storage ring PETRA is mainly used as a booster ring for the electron–proton storage ring HERA. 40% of the PETRA operating time is in stand-by mode, which is used for synchrotron radiation operation. To install an undulator in a straight PETRA section a special 4 m-long vacuum chamber with a keyhole-like cross section was built (HASYLAB, 1994). During booster operation the protons pass the wide part (80 mm) of the chamber. The narrow part of the chamber (14 mm) is moved into the undulator gap for synchrotron radiation operation. The undulator beam has a power density of 500 kW mrad^{-2} (at 60 mA and 12 GeV). This corresponds to a power density of 700 W mm^{-2} at 26.5 m from the source, where the undulator beam exits the storage ring. An angular misalignment of 2 mrad of the electron beam would cause the undulator beam to hit the chamber wall. Finite-element modelling calculations have shown that at full power the beam would melt the copper absorber of the storage ring vacuum chamber within 20 ms. This shows that, for safe and stable operation of the whole beamline, precise and reliable beam-position monitoring is mandatory. Three different types of beam-position monitoring devices are used in the beamline:

(i) Two simple fluorescence screen monitors with copper filters at 50 and 100 m source distance are used to set up the beam visually at low-power operation.

(ii) Two beam-position monitors at 57 and 100 m use photoemission current for fine-steering the beam.

(iii) A graphite foil monitor at 102 m detects that the whole beam passes the front end.

The design of these different types of monitors is strongly influenced by their purpose and the operational needs of beamline and experiments.

2. Injection – closing the gap – fluorescence screens

Undulator operation is possible only when PETRA is not used as an injector for HERA. During that time the beam injection starts at 7 GeV with an open undulator and the wide part of the keyhole chamber in the beam. After injection the particle energy is increased to its final value of 12 GeV. Then the narrow part of the keyhole chamber is moved into the beam to allow for undulator operation. The safety beam shutters at 48 and 104 m have to move to the open position before it is possible to close the undulator gap (the safety shutters are not sufficiently cooled to stop the undulator beam). Now the most critical phase of the beam alignment starts. The beam must pass several narrow parts of the beamline without hitting them. Fig. 1 gives an overview of all the apertures, monitors and windows of the beamline. The first component that is endangered by the beam is the copper crotch of the outlet chamber at 26.5 m, followed by two water-cooled graphite apertures, AP1 and AP2, in the ring tunnel. For the final steering the beam has to pass the centre of the beam-position monitors at 57 (BPM1) and 100 m (BPM2). The fluorescence screen monitors, LM, are used at low currents to visually check the alignments. These fluorescence screens are simple 10 mm-thick copper plates. These can move into the photon beam. The radiation passes the plate under an angle of 45°. The back plane is covered with a fluorescence screen. Fluorescence light from this screen is detected perpendicular to the beam by a video camera and gives a visual impression of the beam position relative to centre marks on the screen. There is enough hard X-ray intensity to use both fluorescence screens simultaneously at 57 and 100 m. The screen images of the beam are used by machine operators to control the beam in position and angle during the machine start-up phase. This is possible without any risk of damage for undulator gaps bigger than 30 mm. Below this gap size the monitors move out of the beam to avoid damage to the fluorescence screen.

3. Beam-position monitors

One of the main experimental requirements is a stable beam position at the sample. The experiments at the PETRA beamline

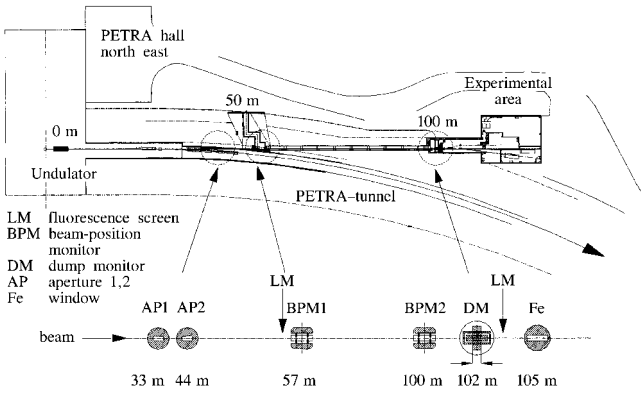

Figure 1
The PETRA beamline with the different monitors.

Table 1
Beam-position monitor parameters.

	Vertical	Horizontal
Blade distance BPM1 at 57 m	4 mm	12 mm
Blade distance BPM2 at 100 m	7 mm	15 mm
Resolution	1 μm	2 μm

need a stability better than 100 μm. To achieve this, beam-position monitoring with a feedback loop to the machine is required.

Two beam-position monitors (Johnson & Oversluizen, 1989) of the DORIS type (HASYLAB, 1990) are installed. At installation distances of 57 and 100 m the power densities are comparable with those at the monitor positions of the DORIS insertion devices. This allows us to use these monitors with slight modifications.

Fig. 2 shows the PETRA beam-position monitor. The central part of the monitor is the water-cooled Cu block (3) which holds and cools the tungsten electrodes (1). The 0.4 mm-thick blades are prealigned and assembled in two monitor modules (5) which are fixed to the cooling block (3). To detect the photoemission current from the blades, electrical insulation is achieved by 0.6 mm-thick AlN plates. The cooling block is attached to

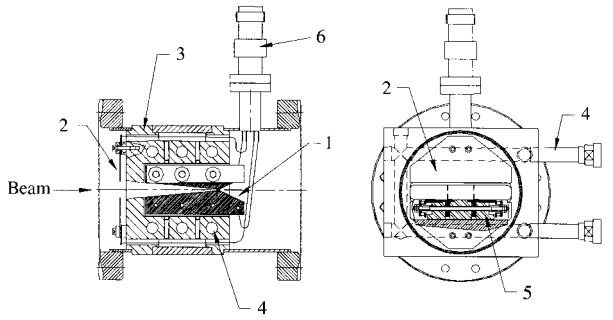

Figure 2
The PETRA beam-position monitor with (1) tungsten electrode, (2) dump electrode, (3) Cu block, (4) cooling channel, (5) monitor module, (6) electrical feedthrough.

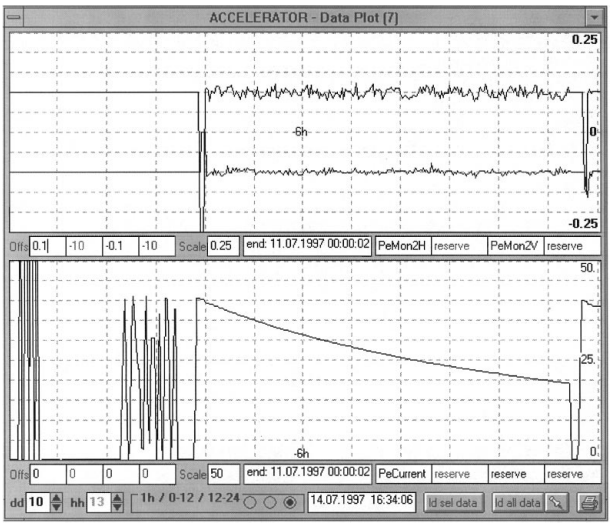

Figure 3
Data plot of the beam position at monitor 2 (100 m). The upper curves show the horizontal and vertical beam position as a function of time. The lower curve is the particle beam current *versus* time.

remote-controlled vertical and horizontal translation stages (not shown in Fig. 2) for calibration purposes. To simplify the alignment of the monitor assembly the reference top plane of the monitor block is aligned parallel to the horizontal axis of the blades. In Table 1 the main features of the PETRA monitors are listed. Fig. 3 shows typical data taken over a period of 12 h for horizontal and vertical beam positions at the second monitor (100 m from the source). The bottom curve shows the beam current *versus* time. The beam-position scale ranges from −0.25 to 0.25 mm. The zero position is arbitrary to separate the curves. The curves show a precision better than 20 μm vertical and 50 μm horizontal. The first 3.5 h of the recorded data show typical booster operation at PETRA.

The main difference from DORIS beam-position monitors is the additional tungsten dump electrode (2), which is mounted in front of the monitor. These tungsten blades protect the Cu block against melting by a misaligned undulator beam. The photoemission from these blades is detected and indicates a vertically misaligned beam.

4. Beam dump – equipment safety

Accidental misalignment of the beam would destroy the storage ring and beamline equipment with severe consequences for the operation of the storage ring and the beamline. A special fail-safe monitor has been designed, which makes use of the photocurrent and the thermal stability of carbon foils in hot X-ray beams. We need this special monitor because equipment melting starts after 20 ms at closed-gap operation. The beam position is stabilized by control cycles of the beam-position monitors (see §3) with a repetition rate of 0.5 Hz. This is two orders of magnitude too slow to prevent equipment melting.

The dump monitor detects the beam at closed-gap operation (gaps smaller than 28 mm). As long as the undulator beam is detected, there is no danger of equipment melting. If no undulator beam signal is detected, the electron beam is dumped within 8 ms. The detector consists of a 1 mm-thick carbon filter and a 30 mm-wide carbon foil, 0.13 mm thick. The carbon filter discriminates between bending-magnet radiation and the undulator beam. A comparison of the PETRA bending-magnet spectrum with two undulator spectra for different gap heights (14 and 28 mm) in Fig. 4 shows the need for this filter. The photoemission of the thin carbon foil (0.13 mm thick) is measured, and a current

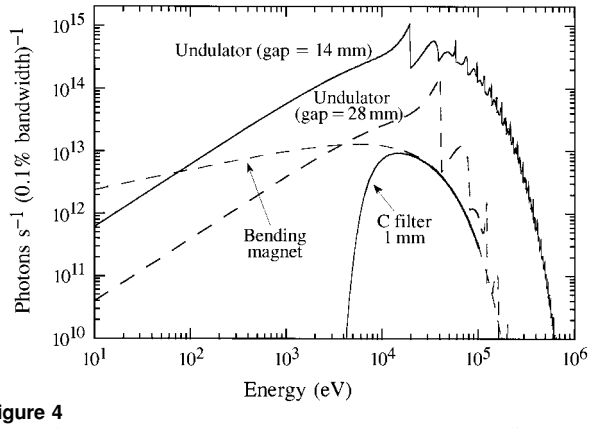

Figure 4
Comparison of the spectral flux of the PETRA undulator at different gaps with the flux of the bending magnet (calculated for 0.8 mrad horizontal width). Additionally shown is the spectrum of the bending magnet filtered by a 1 mm-thick carbon foil.

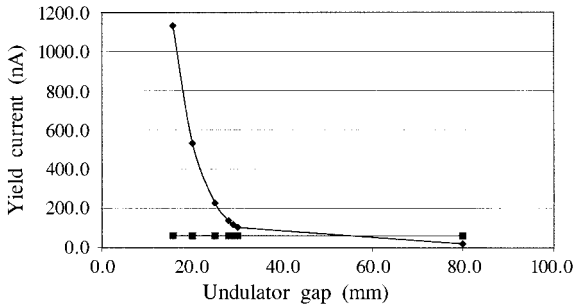

Figure 5
The photoemission current as a function of the gap size (closed diamonds) and installed dump threshold (closed squares). The current of PETRA was 4 mA at an energy of 12 GeV.

threshold, which depends on the stored beam current, determines if the beam is in the correct position. The vertical sensitivity range is restricted to 19 mm by the aperture of the second beam-position monitor. The largest controlled gap of 28 mm is chosen because this gap size gives the power density limit where misalignments of the undulator beam become dangerous for the crotch and other beamline components. When the undulator reaches this gap the closing process stops until the dump monitor detects the beam. The photoemission yield is very high for the lower energetic part of the spectrum. The comparison in Fig. 4 shows that even at 100 m from the undulator source (80 m from the bending magnet) the contribution to the total yield of the bending magnet is higher than that of the undulator. We insert a carbon filter (1 mm thick) between the source and detector foil and cut off the low-energy photons. In this way the undulator dominates the photoemission yield and it is possible to define a reliable threshold for beam detection. Fig. 5 shows a yield curve of the detector foil at 4 mA beam current as a function of the undulator gap. The installed dump threshold is added. For undulator gaps smaller than 28 mm and a yield current below the threshold, the beam is dumped. This system is fail-safe, as a destroyed detector foil would also stop the beam.

5. Conclusions

At the undulator beamline of the storage ring PETRA, several monitors are installed to control the operation of the beam. For visual control, fluorescence screens are used. Photoemission beam-position monitors for fine-steering the beam are used. The achieved beam-position stability at the sample at 130 m source distance is better than 100 μm. A simple graphite-foil monitor has been developed to generate a dump signal in the case of a misaligned, and therefore absent, beam. The installed beam-dump system works reliably and is fail-safe as described. For example, a sudden power supply failure in the machine caused severe misalignments of the beam. The dump monitor detected the misalignment and stopped instantaneously the particle beam and undulator operation.

References

Balewski, K., Brefeld, W., Hahn, U., Pflüger, J. & Rossmanith, R. (1995). *Proceedings of the 16th International Conference on High Energy Accelerators, Dallas, USA*, Vol. 1, p. 275. Piscataway, NJ: APS/IEEE.

Hahn, U., Schulte-Schrepping, H., Balewski, K., Schneider, J. R., Ilinski, P., Lai, B., Yun, W., Legnini, D. & Gluskin, E. (1997). *J. Synchrotron Rad.* **4**, 1–5.

HASYLAB (1990). Annual Report, pp. 125–129. HASYLAB, Hamburg, Germany.

HASYLAB (1994). Annual Report, pp. 110–114. HASYLAB, Hamburg, Germany.

Johnson, E. D. & Oversluizen, T. (1989). *Rev. Sci. Instrum.* **60**(7), 1947–1950.